HYDROLOGICAL PROCESSES
Hydrol. Process. (2015)
Published online in Wiley Online Library
(wileyonlinelibrary.com) DOI: 10.1002/hyp.10641

Modelling temperature change downstream of forest harvest using Newton's law of cooling

Lawrence J. Davis,[1] Maryanne Reiter[2]* and Jeremiah D. Groom[3]

[1] *D3 Scientific, Springfield, OR, USA*
[2] *Weyerhaeuser Company, Springfield, OR, USA*
[3] *Oregon State University, Corvallis, OR, USA*

Abstract:

We adapted Newton's law of cooling to model downstream water temperature change in response to stream-adjacent forest harvest on small and medium streams (average 327 ha in size) throughout the Oregon Coast Range, USA. The model requires measured stream gradient, width, depth and upstream control reach temperatures as inputs and contains two free parameters, which were determined by fitting the model to measured stream temperature data. This model reproduces the measured downstream temperature responses to within 0.4 °C for 15 of the 16 streams studied and provides insight into the physical sources of site-to-site variation among those responses. We also use the model to examine how the pre-harvest to post-harvest change in daily maximum stream temperature depends on distance from the harvest reach. The model suggests that the pre-harvest to post-harvest temperature change approximately 300 m downstream of the harvest will range from roughly 82% to less than 1% of that temperature change that occurred within the harvest reach, depending primarily on the downstream width, depth and gradient. Using study-averaged values for these channel characteristics, the model suggests that for a stream representative of those in the study, the temperature change approximately 300 m downstream of the harvest will be 56% of the temperature change that occurred within the harvest reach. This adapted Newton's law of cooling procedure represents a highly practical means for predicting stream temperature behaviour downstream of timber harvests relative to conventional heat budget approaches and is informative of the dominant processes affecting stream temperature. Copyright © 2015 John Wiley & Sons, Ltd.

KEY WORDS stream temperature; Newton's law of cooling; downstream; timber harvest; temperature modelling

Received 19 May 2015; Accepted 9 August 2015

INTRODUCTION

Stream temperature change due to forest harvest has been widely studied at both local scales (e.g. Gray and Edington, 1969; Brown and Krygier, 1970; Baillie *et al*., 2005; Gomi *et al*., 2006; Gravell and Link, 2007; Groom *et al*., 2011a, b; Janisch *et al*., 2012; Rex *et al*., 2012; DaSilva *et al*., 2013; Kibler *et al*., 2013) and downstream scales (Brown *et al*., 1971; Caldwell *et al*., 1991; Zwieniecki and Newton, 1999; Story *et al*., 2003; Rutherford *et al*., 2004; Cole and Newton, 2013; Garner *et al*., 2014; Johnson and Wilby, 2015). This abundance of studies reflects the concern over stream temperature impacts to aquatic ecosystems and has led to the evolution of stream protection rules for managed forests (e.g. Hairston-Strang *et al*., 2008). In the Pacific Northwest, studies have shown that contemporary forest practices (e.g. Groom *et al*., 2011a,b) produce less warming on fish-bearing streams relative to earlier practices (e.g. Brown and Krygier, 1970), yet there remains concern over downstream thermal impacts. In their review of timber harvest effects on stream temperature, Moore *et al*. (2005) found that only a few of the numerous studies they reviewed attempted to quantify the processes governing water temperature as it flows downstream (Brown *et al*., 1971; Story *et al*., 2003; Johnson, 2004). They go on further to say 'Clearly, more research is required to clarify the mechanisms responsible for downstream cooling and how they respond to local conditions'.

Several studies examining downstream temperature response found general cooling trends as streams enter well-shaded reaches (e.g. Caldwell *et al*., 1991; Zwieniecki and Newton, 1999; Story *et al*., 2003), although both the direction and magnitude of temperature changes within individual streams are variable (e.g. Cole and Newton, 2013). Of the studies measuring downstream temperature, a few have attempted to quantify the mechanisms responsible for the observed variability in downstream responses. For example, some studies

*Correspondence to: Maryanne Reiter, Weyerhaeuser Company, 785 N 42nd St, Springfield, OR 97478, USA.
E-mail: maryanne.reiter@weyerhaeuser.com

Copyright © 2015 John Wiley & Sons, Ltd.

indicate that groundwater is an important component of observed cooling (e.g. Brown *et al*., 1971; Story *et al*., 2003), while others observed cooling in the absence of significant groundwater or tributary input (Cole and Newton, 2013; Garner *et al*., 2014). Achieving predictability in the physical processes governing reach-scale downstream temperature response to forest harvest and other events that reduce riparian canopy cover is an important step in understanding the thermal behaviour of streams at the watershed scale.

Modelling and predicting downstream temperature dynamics often rely on heat or energy budgets, which use a suite of at-a-site or proximal parameter values to quantify heat fluxes into and out of a stream (e.g. Brown, 1969; Sugimoto *et al*., 1997; Boyd and Kasper, 2003; Roth *et al*., 2010). These heat budget models are useful in determining the relative contributions of channel, stream-adjacent and atmospheric parameters to stream temperature and give insight into the mechanisms behind those factors (e.g. heat source; Boyd and Kasper, 2003). However, widespread practical application of these models may be hindered by their need for accurate measurement of a suite of site-specific parameters, many of which are often not available (Johnson and Wilby, 2015). Efforts to quantify these site-specific parameters necessary for estimating the heat flux components governing downstream temperature response have used combined reach-scale micrometeorological, hydrological and stream temperature measurements (e.g. Roth *et al*., 2010; Garner *et al*., 2014). While these studies provide deep insight into processes occurring at a reach scale, the measurements they require are difficult and costly to repeat across the landscape. In contrast, a calibrated Newton's law of cooling (NLC) model may also provide process-level insights and predictive power while requiring fewer and more readily obtained parameter measurements. The goals of this study are to (1) build a practical physical model that requires a minimum number of measured stream properties as inputs and (2) use the physical model to explain the individual temperature change behaviours of specific sites directly from their physical properties. The data we utilized are from a subset of Oregon Coast Range streams used in a previous study examining the effect of forest harvest on stream temperature (Dent *et al*., 2008; Groom *et al*., 2011a,b). We combined these data with readily measured stream characteristics to quantitatively analyse and predict pre-harvest to post-harvest temperature changes in the unharvested, high-shade reaches downstream of harvested reaches with buffers. This approach helps to clarify the mechanisms responsible for downstream cooling as called for by Moore *et al*. (2005) and provides an approach that might be adapted to investigate downstream processes across larger geographic regions.

FUNDAMENTAL PHYSICS OF STREAM TEMPERATURE DYNAMICS

In order to provide a basis of understanding of the physical principles used in our model, we first review some key fundamentals. *Equilibrium temperature*, denoted by T_{eq}, is the temperature at which the sum of all thermal energy fluxes (net flux) into the stream is zero ($\sum q = 0$). The difference between the temperature of an object and its equilibrium temperature determines the direction and rate of heat flux to/from an object. Objects will have either positive (heating) or negative (cooling) heat flux such that the temperature will trend towards T_{eq}. *Heat capacity*, denoted as C, quantifies the resistance of the object to temperature change and is calculated as the mass of the object multiplied by the specific heat of the material comprising the object. The rate of temperature change of the object will then be $\sum q/C$. For the specific case of water flowing in a stream, the net heat flux and T_{eq} depend on the stream and environmental temperatures in addition to the stream morphology, shade, stream bed material and all other factors influencing heat flux components in the area. Consequently, the temperatures of the stream water and the surrounding thermodynamic environment are not constant, resulting in a T_{eq} that also is not constant. The commonly observed diurnal stream temperature oscillations are a result of the stream water continuously trending towards this diurnally oscillating T_{eq}.

The processes involved in thermal energy exchange in a stream have been thoroughly discussed elsewhere (Edinger *et al.*, 1968; Adams and Sullivan, 1989; Bogan *et al*., 2003; Caissie, 2006), and we only briefly re-introduce them here for the purpose of establishing a basis of comparison with our model. The basic factors influencing the total rate of energy transfer (q) into or out of a stream can be expressed as follows:

$$\sum q = q_{radiation} + q_{mixing} + q_{convection} + q_{conduction} \quad (1)$$

Here, $q_{radiation}$ includes the heat flux due to solar and blackbody radiation; q_{mixing} includes both surface and groundwater inputs; $q_{convection}$ includes the heat flux due to conduction–convection and evaporation–convection; and $q_{conduction}$ includes bed conduction. When $q_{radiation}$ and q_{mixing} are minimized because of high shading and few tributaries or groundwater sources, then the conduction and convection contributions to $\sum q$ dominate the total rate of energy transfer into or out of a stream. In this case, NLC may accurately describe the temperature behaviour of the system. NLC, described by Equation (2), is an empirical relationship, which states that the rate of temperature change of an object is proportional to the difference between the object temperature and the

Copyright © 2015 John Wiley & Sons, Ltd.

temperature with which the object is equilibrating (T_{eq}). Despite the name, NLC also properly accounts for positive $\frac{dT}{dt}$ (warming) when ($T < T_{eq}$) as can be seen from Equation (2) in the following:

$$\frac{dT}{dt} = \alpha\left(T_{eq} - T\right) \tag{2}$$

The temperature decay coefficient (α) in the preceding equation is given by $\alpha = hA/C$, where A is the surface area across which heat is exchanged, C is the heat capacity of the object and h is the heat transfer coefficient, which describes the ease with which an object exchanges heat with its environment. For the specific case of a *constant* equilibrium temperature, the solution to Equation (2) is the integrated form of NLC:

$$T(t) = T_{eq} + \left[T_0 - T_{eq}\right]e^{-\alpha t} \tag{3}$$

A previous work has shown that $q_{radiation}$ may be so reduced within heavily shaded reaches that it no longer dominates the net heat flux (e.g. Garner *et al.*, 2014). Considering this result, we hypothesized that for sections of streams that are sufficiently shaded and lacking tributaries, the $q_{radiation}$ and q_{mixing} contributions to $\sum q$ may be so reduced relative to $q_{convection}$ and $q_{conduction}$ that NLC becomes applicable. We tested this hypothesis by applying an NLC-based model to predict temperature changes in the heavily shaded downstream study reaches that did not have significant surface water inputs from tributaries. We assumed that any groundwater mixing would be relatively constant from before to after forest harvest.

Finally, an important concept in discussing downstream temperature behaviour is the measurement frame of reference. Stream temperature is typically measured in the Eulerian frame of reference, which is based on measuring the value of parameters in a spatially bounded location (Doyle and Ensign, 2009). In the Eulerian frame, a temperature sensor is stationary, and the stream flows past it. A time series of temperature at a specific location in the Eulerian frame is produced by measuring temperatures at successive instances in time, and thus, each temperature measurement is made on a different volume of water. The Lagrangian frame, in contrast, is a reference frame attached to a specific volume of water as it travels downstream. In the Lagrangian frame, the water parcel is continuously arriving in new environmental conditions, and stream temperature is measured always within the same parcel at different instances in time (and thus at different locations within the Eulerian frame).

The use of the terms *heating* and *cooling* without specification of the reference frame in which these changes in temperature are measured can be a source of confusion and misconception because the observed condition of heating or cooling as measured in one frame does not necessarily coincide with a temperature change in the same direction as observed in the other frame. For example, a parcel of water may travel through an upstream, low-shade reach, warming along the way, before passing into a high-shade reach. Within the downstream reach, the parcel may continue to warm, likely at a significantly decreased rate. A later measurement of the parcel temperature would indicate downstream heating in the Lagrangian frame, because parcel temperature monotonically increased with time. However, while this first parcel was in transit through the downstream reach, solar radiation may have increased during the diurnal cycle so that a second parcel passing through the low-shade upper reach might warm at such a high rate relative to the first parcel, currently in the shaded reach and largely unaffected by the increase in solar radiation, that the second parcel temperature becomes greater than that of the first parcel. At this instant in time, the temperature measured at the downstream location would be less than the temperature at the upstream location; thus, measurement in the Eulerian frame would indicate stream cooling. Here, we see the direct contradiction in temperature change as measured in the two different reference frames.

In order to avoid future confusion, we suggest specifying either Lagrangian or Eulerian heating and cooling when describing stream temperature changes (e.g. Rutherford *et al.*, 2004). Within this paper, we will only use the terms heating and cooling in reference to the Lagrangian frame. The Lagrangian frame is more naturally suited to modelling cause-and-effect behaviour in stream temperature dynamics because it tracks how the temperature of fluid in motion changes over time as it encounters new thermodynamic environments. In contrast, the Eulerian frame compares the temperature of two different parcels of water at an instant in time, and those two parcels may have experienced completely different and causally detached thermodynamic environments up to that point. In order to compare predictions provided by a Lagrangian model to data taken in the Eulerian frame, the transit time for parcels of water between Eulerian locations must be measured or modelled. The transit time information allows for Eulerian frame temperature measurement at a specific time and location to be attributed to the temperature of a specific parcel of water arriving at that location at that time. The term advection is often introduced to describe this transport of thermal energy from one Eulerian location to another via stream flow. However, we see that the effects of advection are intrinsically included in a Lagrangian frame model. In fact, for continuous flow situations without significant pooling or

Copyright © 2015 John Wiley & Sons, Ltd.

recirculation, the values in a time series of temperatures measured in the Eulerian frame are the temperatures, tracked in the Lagrangian frame, of successive parcels of water arriving at that location.

DATA COLLECTION METHODS

The pertinent information on field data collection for this analysis is described later. A full description of data collection and field protocols can be found in Groom *et al*. (2011b); also see Dent *et al*. (2008) for a map of the study area and full description of site selection criteria and Groom *et al*. (2011a) for a summary of the forest harvest reach site characteristics including channel and riparian vegetation statistics pre-harvest and post-harvest. The criteria for stream selection included no beaver influence (dams with ponds or disturbed vegetation), average annual flow rates of 283 l/s or less and treatment reaches harvested according to state and private forest prescriptions for fish-bearing streams, which require varying amounts of overstory tree retention depending on ownership and stream size.

Programmable, waterproof data loggers (referred to as 'probes' in this paper; 'W' indicates water probes as opposed to air probes) were installed in control reaches upstream of forest harvest (Figure 1; reach between probes 1W and 2W). These control reaches were established to provide a measure of year-to-year and spatial variability in stream temperature that occurs independent of harvest. The treatment reach (Figure 1; reach between probes 2W and 3W) was established to quantify stream temperature changes due to forest harvest. The downstream reach (Figure 1; reach between probes 3W and 4W) was established to examine potential downstream temperature responses to any temperature changes occurring within the harvest unit (Figure 1). The downstream reach was approximately 180 to 345 m below the treatment reach and had to be relatively homogeneous with intact riparian vegetation and no major tributaries in order to minimize confounding variables including mixing. These criteria resulted in only 18 of the 33 study sites having a downstream reach. Hourly stream temperature was monitored for 2 years before timber harvest and 5 years after harvest between 1 June and 30 September. Other data collected for the study include maximum stream depth, bank full and wetted width, shade and stream gradient. These parameters were measured within each reach at 60-m intervals. Channel metrics were collected according to Kaufmann and Robison (1998). Hemispherical photographs were taken using a self-levelling fish-eye camera 1 m above the stream surface using the protocol according to Valverde and Silvertown (1997). Solar radiation indices based on latitude, longitude and elevation were derived from these photographs using HemiView® software version 2.1 (Delta-T Devices, Ltd, Cambridge, UK). Shade was estimated by $1 - GSF$, where GSF (global site factor) is the ratio of direct plus diffuse solar power below canopy to direct plus diffuse power above canopy. Further detail on the processing of these data is described in Groom *et al*. (2011a).

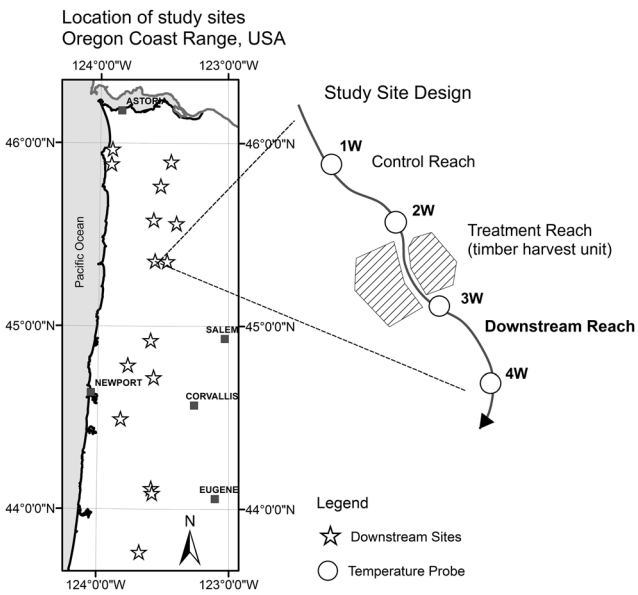

Figure 1. Location of study sites in the Oregon Coast Range. Inset shows field study design with relative locations of control, harvest and downstream reaches indicated. Temperature probes 1W and 2W are above and below the control reach, respectively; probe 3W is below the harvest reach; and probe 4W is approximately 300 m below the harvest reach

For this analysis, data from the summer immediately before and immediately after harvest were used. If data from only one of the immediate pre-harvest or post-harvest years were not available, then data from the next adjacent year were used for this analysis (e.g. 2 years pre-harvest or 2 years post-harvest). Sites with two consecutive years of unavailable data on either side of harvest were not used. As a result of these temporal data constraints, 16 of the 18 downstream sites were used in this analysis. The sites used in this analysis were an average of 5.0 m wide (range = 2.8–7.0 m) with a mean watershed area of 327 ha (range = 80–692 ha). The temperature metric analysed in this paper was the 40-day mean of maximum daily temperature computed from the daily maximum values from 15 July to 23 August. This metric was chosen because it aligns with a previous study using the same metric computed from these same data (Groom *et al*., 2011b). In contrast to Groom *et al*. (2011a,b), this work focuses on the downstream data. Specifically, this paper describes application of an NLC model to understand the dependence of downstream pre-

Copyright © 2015 John Wiley & Sons, Ltd.

AGENDA ITEM F
Attachment 2
Page 4 of 13

harvest to post-harvest change in maximum temperature on change in harvest reach maximum temperature, as well as measured downstream stream properties and distance downstream of the harvest reach.

NLC MODEL DEVELOPMENT

Initial assumptions

We first assume that a parcel of water moving downstream in a highly shaded reach will follow NLC, and thus, the rate of temperature change for the parcel will be proportional to the difference between the parcel temperature and its unknown, environmentally influenced, equilibrium temperature. The equilibrium temperature may be correlated with, but is not entirely represented by, the temperature of any particular entity in the stream environment. Rather, the equilibrium temperature is a weighted average of the temperatures of all environmental entities with which the stream exchanges energy, with the weights being the rate at which energy can be exchanged with each entity. Therefore, the equilibrium temperature is constantly changing on diurnal and seasonal time scales.

To apply NLC to streams, the conditions that T_{eq} and α are constant require that the transit time, τ, is small compared with the time over which the downstream T_{eq} and α change appreciably. Thus, the reach length over which the NLC model is applied must be sufficiently short and/or fast flowing to meet the constant T_{eq} and α conditions (Rutherford *et al.*, 2004). When using NLC to model a parcel of flowing water, the value of hA is anisotropic (dependent on direction) because the horizontal surface area is greater than the vertical surface area (e.g. the streams are wider than they are deep) and heat is exchanged with different materials by various different mechanisms in different directions, for example, conduction into the stream bed in the downward direction and convection with the air in the upward direction. To account for these complexities, we defined the effective decay coefficient, $\alpha' = \gamma/C$, where γ is the sum of the different hA terms for each direction.

One of the primary goals of this study was to reduce the number of stream parameters required for a predictive model; thus, the stream data necessary to accurately calculate the values of T_{eq} and γ from first principles were not provided by this study. Instead, the pre-harvest to post-harvest change in T_{eq} will be modelled using changes in control reach temperature, resulting in the first free parameter of the model, and γ will be incorporated into the second of the two free parameters. The values of the two free parameters in our NLC model are determined by fitting the model to the measured changes in maximum downstream temperature. However, we will show that for the set of streams used in this study, the free parameters are not *necessarily* site specific, and the lack of a priori calculation of T_{eq} and γ does not prevent the NLC model from accurately describing changes in maximum downstream temperatures between pre-harvest and post-harvest summers.

Applying the integrated NLC

First, we apply Equation (3) to a parcel of water in transit through the un-harvested downstream reach, between temperature probes 3W and 4W, as indicated in Figure 1. Setting $t = 0$ when the parcel passes temperature probe 3W at the end of the harvest reach and τ equal to the transit time between temperature probes 3W and 4W allows conversion from the Lagrangian frame to the Eulerian (thermistor data) frame. The correspondence between terms in Equation (3) and terms in the stream temperature model becomes $T3W \rightarrow T\,(t = 0)$, $T4W \rightarrow T\ (t = \tau)$ and $T_{eq} \rightarrow T4W_{eq}$, where $T4W_{eq}$ represents the equilibrium temperature in the downstream reach, and finally, $\alpha \rightarrow \alpha'$ as discussed previously. Making these substitutions in Equation (3), we arrive at

$$T4W = T4W_{eq} + \left[T3W - T4W_{eq}\right] e^{-\alpha' \tau} \qquad (4)$$

This model treats the temperature measured at a specific probe location in the Eulerian frame as equal to the temperature of the water parcel passing over the probe at that time, which is modelled in the Lagrangian frame. This model also treats T_{eq} as constant in space across the downstream reach and constant over the transit time (τ). As discussed previously, this assumption requires that τ is small compared with the time over which $T4W_{eq}$ and α' change appreciably and that the length of the downstream reach is small compared with the distance over which $T4W_{eq}$ and α' change appreciably (Rutherford *et al.*, 2004). Consequently, application of the model is restricted to ≈300 m, downstream of the harvest reach. Within this distance, shade values do not vary significantly, and the transit time is on the order of only 1 h, as indicated by an average flow speed of 0.1 m/s computed from dye-based velocity measurements performed on a subset of representative streams.

Deriving the across-harvest temperature change

The measured change in downstream temperature across the harvest period ($\Delta T4W$) is determined by subtracting $T4W$ during the summer prior to harvest from $T4W$ during the summer after harvest. This results in Equation (5).

Copyright © 2015 John Wiley & Sons, Ltd.

$$\Delta T4W = T4W_{post} - T4W_{pre} \quad (5)$$

With $T4W$ modelled by Equation (4) and given that downstream $T4W_{eq}$, α and τ in the un-harvested downstream reach are unaffected by the upstream harvest, the NLC model for Equation (5) becomes

$$T4W_{eq,post} + \left[T3W_{post} - T4W_{eq,post}\right]e^{-\alpha'\tau} - T4W_{eq,pre} + \left[T3W_{pre} - T4W_{eq,pre}\right]e^{-\alpha'\tau} \quad (6)$$

With some algebraic simplification, the change in downstream temperature $\Delta T4W$ can be written as follows:

$$\Delta T4W = \Delta T3We^{-\alpha'\tau} + \Delta T4W_{eq}\left[1 - e^{-\alpha'\tau}\right] \quad (7)$$

Here, $\Delta T3W$ and $\Delta T4W_{eq}$ are the across-harvest-year changes in temperature at the 3W probe and in the downstream reach equilibrium temperature, respectively. Within this model, the stream properties serving as the primary drivers of the measured variations in $\Delta T4W$ do so via their influence on α' and τ. Modelling the dependence of α' and τ on the site-specific stream properties allows for prediction of the measured variation in $\Delta T4W$ among the study streams.

Downstream transit time. The transit time of the downstream reach is modelled as $\tau = L/v$, where L is the downstream reach length and v is the flow speed in the downstream reach. We do not have direct flow speed measurements for all streams in the downstream reach, so we modelled the flow speed using gradient measurements together with Manning's formula (Subramanya, 2009), which states that $v \propto G^{1/2}$, resulting in Equation (8):

$$\tau \propto \frac{L}{G^{1/2}} \quad (8)$$

Here, G is the average gradient of the stream within the downstream reach, typically defined as length along the stream divided by change in elevation. The site-specific G values used in the model are an average of these gradient measurements for each downstream reach.

Heat capacity of the stream. The heat capacity (C) of the modelled parcel of water is proportional to the volume of the parcel and consequently the cross-sectional area of the stream. For streams approximated as triangular or trapezoidal, the volume is proportional to the maximum depth (D) multiplied by the wetted width (W). We use the average measurements W and D for each downstream reach (Equation (9)).

$$C \propto W\,D \quad (9)$$

Downstream shade factor. Shade and shelter provided by stream-side vegetation and local topography reduce solar heating during the day and radiative cooling at night and also reduce wind speed, and consequently conduction–convection and evaporation–convection. We hypothesize that through these processes, the level of downstream vegetation may influence the downstream temperature response to forest harvest. The site-specific downstream shade factor (S) was derived from the global site factor as discussed in the Section on Methods. However, uniformity in the un-harvested downstream canopy among the study streams produced a small range of S values (0.83 to 0.96), which was not sufficient to significantly affect the predictions of the model. This result suggests that a study incorporating a wider range of downstream canopy densities would be needed in order to provide the information required to evaluate and validate a downstream shade component in the model, as discussed further in the Section on Modelling Discussion.

Integrating site specificity

The dominant stream properties driving variation in $\Delta T4W$ are incorporated into our model by combining Equations (8) and (9) to arrive at

$$\alpha'\tau \propto \varphi\frac{L}{WDG^{1/2}} \quad (10)$$

Here, φ is a model parameter incorporating the proportionality constants associated with Equations (8) and (9). Given limited environmental and stream data, we initially assume that φ is approximately non-site specific for the streams in this study, which is supported by the success of the model when a general φ value is used.

Downstream equilibrium temperature. Finally, we model the yet-unknown changes in downstream equilibrium temperature ($\Delta T4W_{eq}$), which are not harvest related (e.g. climatic). Our model requires only the change in equilibrium temperature, so we are not forced to attempt a calculation of the absolute equilibrium temperature both pre-harvest and post-harvest. Instead, we use pre-harvest to post-harvest changes in the stream temperature measured at probes 1W and 2W, which lie upstream from harvest, to estimate $\Delta T4W_{eq}$ directly. In the context of our NLC model, year-to-year changes in the local climate will influence actual stream temperature by changing T_{eq}. From Equation (7), we see that the rate at which the change in downstream temperature varies as equilibrium temperature varies, $\frac{d(\Delta T4W)}{d(T4W_{eq})} = 1 - e^{-\alpha'\tau}$, is

Copyright © 2015 John Wiley & Sons, Ltd.

constant for a given α' and τ', corresponding to a specific site. This result suggests that within the confines of this model, changes to T_{eq} cause proportional changes to stream temperature, so we approximate changes in the control reach temperatures, $\Delta T1W$ and $\Delta T2W$, as proportional to changes in the control reach equilibrium temperatures, $\Delta T1W_{eq}$ and $\Delta T2W_{eq}$. In order to connect these control reach changes, $\Delta T1W_{eq}$ and $\Delta T2W_{eq}$, to changes in $\Delta T4W_{eq}$, we assume that local changes in climate will affect the control reach and downstream reach equilibrium temperatures differently, but proportionally, so that $\Delta T4W_{eq}$ is modelled as

$$\Delta T4W_{eq} = \beta \Delta T_{1W,2W} \tag{11}$$

Here, $\Delta T_{1W,2W}$ is the average of $\Delta T1W_{eq}$ and $\Delta T2W_{eq}$. The proportionality constant β is the second free parameter in the NLC model and is determined from fitting the model to measured stream temperature data.

Complete NLC model

To arrive at the complete NLC model, we insert Equations (10) and (11) into Equation (7), giving the model equation:

$$\Delta T4W = \Delta T3W e^{-\varphi \frac{L}{WDG^{1/2}}} + \beta \Delta T_{1W,2W}\left[1 - e^{-\varphi \frac{L}{WDG^{1/2}}}\right] \tag{12}$$

We then model the expected $\Delta T4W$ using the measured upstream temperature changes, downstream reach length and average values for gradient, wetted width and maximum depth with Equation (12). In the following section, we apply this model to data from the study sites in order to understand the underlying causes of the downstream temperature responses exhibited by individual streams and the variability among those responses. We estimate parameter values for β and ϕ using a nonlinear least squares regression procedure in Program R (The R Foundation for Statistical Computing, version 3.1.2, 2014). We compared the performance of the nonlinear model with a linear fit of the regression equation:

$$\Delta T4W \sim \Delta T3W + \varepsilon \tag{13}$$

Performance was evaluated by examining model root-mean-square-error (RMSE) terms and small-sample adjusted Akaike's information criterion values (AIC_c; Burnham and Anderson, 2002). We additionally examined model overfitting and individual point influence on parameter estimates by conducting a leave-one-out cross-validation (LOOCV) procedure. In the procedure, we sequentially re-ran the nonlinear least squares regression with a different individual site removed and used the resulting model to impute the missing $\Delta T4W$ value. We calculated an RMSE statistic from the imputed values.

MODELLING RESULTS

As a basis of comparison with the NLC model results, we first present a simple linear model of the relationship between $\Delta T3W$ and $\Delta T4W$ to test if (i) a model that only depends on harvest reach temperature change is sufficient to explain the variation in the downstream response and (ii) if applying NLC to the data helps explain more of the variation (Figure 2). While the linear regression does describe the general trend in the data, it does not capture the variability in the data or provide insight into the underlying sources of this variation. The linear regression produced an R^2 value of 0.54 and is described by the function

$$\Delta T4W\ (^\circ\mathrm{C}) = [(0.5)\Delta T3W - 0.041](^\circ\mathrm{C}) \tag{14}$$

The slope of the best fit line indicates that for forested streams of the type selected for this study, the pre-harvest to post-harvest change in maximum temperature at a location approximately 300 m downstream of harvest will be, on average, 50% of that change at the harvest location.

Using the fitting procedure discussed in the previous section, we determined the model parameter values $\varphi = 2.2 \times 10^{-4}$ m ($SE = 3.8 \times 10^{-5}$) and $\beta = 1.1$ ($SE = 0.23$) by a two-parameter nonlinear least squares regression (with starting values of 0.001m for φ and 1.5 for β). *RMSE* and AIC_c values indicate that the NLC model better accounts for observed variability, a result also

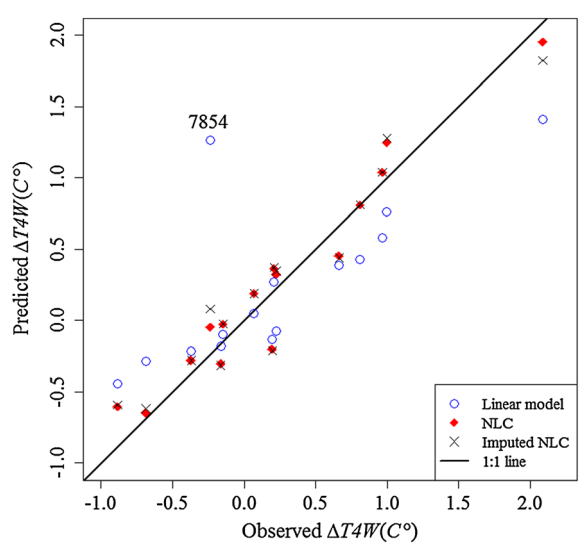

Figure 2. Observed and predicted values of $\Delta T4W$ for the linear regression model (open circles) and the Newton law of cooling model (diamonds). The 1 : 1 line is presented for visual model assessment. Imputed data values from a leave-one-out procedure are indicated by a black 'X'

Copyright © 2015 John Wiley & Sons, Ltd.

indicated by comparing observed *versus* predicted values in Figure 2. The *RMSE*s for the linear model and the NLC model were 0.48 and 0.18, respectively. Similarly, $AIC_c = 28.7$ for the linear model and -1.6 for the NLC model, indicating substantially greater support for the NLC model (Burnham and Anderson, 2002). The LOOCV procedure results in an *RMSE* value of 0.21, and imputed results (Figure 2) indicate that no particular point is driving the fit of the model or disproportionally influencing the free parameter values.

We see that the two-parameter NLC model outperforms the linear regression model at predicting the measured $\Delta T4W$ values, despite having the same number of free parameters (two). In Table I, the differences between modelled and measured $\Delta T4W$ values are all $\leq 0.4\,^{\circ}\mathrm{C}$ in magnitude, with the exception of site 7353. At this site, $\Delta T1W$, $\Delta T2W$ and $\Delta T3W$ (harvest reach) were all negative, and yet $\Delta T4W$ was positive. We therefore conclude that the increase in downstream temperature was not caused by harvest, but rather by some as-yet-unknown local effect occurring in the downstream reach. The model uses temperature data taken upstream of the harvest reach to account for the effects of non-harvest-related temperature fluctuations and thus cannot account for the behaviour of this site because of the localized nature of the downstream disturbance. Considering this result, site 7353 was not included in the fitting procedure used to determine φ and β; a model predicted value of $\Delta T4W$ for this site is not shown in Table I, and model data for this site are not shown in subsequent figures.

We quantify the relative rates at which the pre-harvest to post-harvest change in the temperature will diminish with distance travelled in the downstream reach at each site by removing the effect of the varying reach lengths. The exponent in the NLC model is normalized to the reach length L, and we calculate $(\alpha'\tau)/L = \varphi/[WDG^{1/2}]$. Relatively large values of $(\alpha'\tau)/L$ indicate that the magnitude of the temperature changes measured at a specific downstream locations will decrease in a shorter distance downstream compared with sites with small values of $(\alpha'\tau)/L$. Table I provides the site-specific values of $(\alpha'\tau)/L$. In order to further understand how the distance dependence of $\Delta T4W$ results in the observed values, the site-specific reach length, L, in Equation (12) is replaced with a general distance variable, x, to arrive at an expression for the distance dependence of a change in downstream temperature:

$$\Delta T4W(x) = \Delta T3We^{-\varphi\frac{x}{WDG^{1/2}}} + \beta\Delta T_{1W,2W}\left[1 - e^{-\varphi\frac{x}{WDG^{1/2}}}\right] \tag{15}$$

The range of behaviours produced by the variation in $(\alpha'\tau)/L$ are illustrated in Figure 3, which shows the calculated distance profiles of the downstream pre-harvest to post-harvest temperature change $\Delta T4W(x)$, along with

Table I. ISummarization of sites' experimental ΔT_{4W} values,[a] model error in predicting ΔT_{4W},[b] specific ΔT_{4Weq} values[c] and values of $\alpha'\tau/L$[d]

Site number identifier	$\Delta T4W$ (°C)	Model error	$\Delta T4W_{eq}$ (°C)	$\alpha'\tau/L$ (m^{-1})
5102	−0.37	−0.09	−0.22	0.0026
5104	0.22	−0.10	0.75	0.0021
5201	−0.89	−0.28	−0.36	0.0021
5205	2.09	0.13	0.54	0.0017
5206	1.00	−0.25	0.59	0.0015
5207	0.81	0.00	0.48	0.0011
5301	0.21	−0.16	−0.14	0.0016
5302	0.07	−0.12	0.20	0.0017
5502	−0.15	−0.12	0.25	0.0011
5506	0.66	0.21	0.22	0.0036
5556	0.97	−0.07	−0.64	0.0006
5558	0.20	0.40	−0.21	0.0042
7353[e]	0.86	—	—	—
7801	−0.16	0.14	−0.31	0.0056
7803	−0.69	−0.04	−0.67	0.0119
7854	−0.24	−0.19	−0.29	0.0078

[a] Calculated as the difference between T_{4W} measured before and after harvest.
[b] Measured value subtracted from NLC model values.
[c] Calculated using the NLC model determined parameter value $\beta = 1.1$.
[d] Calculated using the NLC model determined parameter value $\varphi = 2 \times 10^{-4}$ m.
[e] This site was not included in the model; see Section on Modelling Discussion.

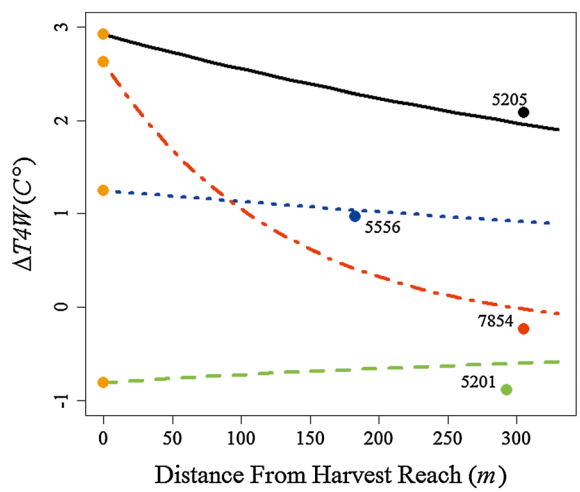

Figure 3. Change in temperature downstream of harvest reach, calculated as a function of distance from harvest reach using the Newton law of cooling model $\Delta T4W(x)$ for several example study sites (lines). Orange dots are measured temperature change at zero distance downstream, $\Delta T4W(x=0) = \Delta T3W$, and coloured dots are measured values of $\Delta T4W(x=L)$ for each site. In all cases, model parameter values were $\varphi = 2.2 \times 10^{-4}$ m and $\beta = 1.1$, and site-specific values of WD, G and $\Delta T_{1,2}$ were used

Copyright © 2015 John Wiley & Sons, Ltd.

the measured $\Delta T4W$ ($x = L$) data for a representative sample of the study streams. Note that these curves and measured data are not plots of the absolute stream temperature as a function of downstream location, but rather plots of the *change* in stream temperature from pre-harvest to post-harvest as a function of downstream location ($\Delta T4W(x)$).

MODELLING DISCUSSION

Model specificity

We see in Figure 2 that the $\Delta T4W$ data deviate from the simple linear model, suggesting that the across-harvest $\Delta T3W$ may not be the only source of the measured variation in across-harvest $\Delta T4W$ and that the behaviour of any particular site can be quite different from the overall behavioural trend. The NLC model we have applied predicts this site-specific variation, indicating a significant deterministic contribution to the variation, as originally hypothesized.

Model generality

The ability of the model to reproduce the measured downstream responses using non-site-specific values for model parameters φ and β indicates that these values are relatively constant across the streams selected for this study. This result further suggests that once these parameters values are determined by fitting of model to data for a given type of stream in a given geographic region, the model might be used to predict the future downstream response to harvest of similar streams in that region. This NLC model does not explicitly treat hyporheic flow or groundwater exchange; however, the effects of these processes on the stream temperature change are implicitly included in the fitted model parameter φ. The fact that φ was held constant in this study suggests that these effects are roughly equally influential across the streams in the study, to within the resolution of this model. The value of $\beta = 1.1$ suggests that for the specific types of reaches examined in this study, the downstream reach equilibrium temperature responds to changes in climatic conditions with roughly equivalent sensitivity to that exhibited by the upstream reaches, to within the resolution of this model.

Model predictive power

The NLC model allows for intuitive analysis of stream sites, which might appear to have outlying behaviour. For example, site 7854 (indicated in Figure 3) experienced a $-0.2\,^{\circ}$C change in downstream temperature even though the harvest reach temperature experienced a relatively large measured temperature increase of $2.6\,^{\circ}$C. The model was able to predict that this site would behave well outside of the general trend defined by other sites, even when this site was not included in the LOOCV parameter determination procedure, as indicated by the proximity of its imputed value relative to its observed value, as seen in Figure 2. Examination of the stream variables in the context of the NLC model reveals that site 7854 experienced an overall decrease in the local equilibrium temperature, as seen in Table I and indicated by negative upstream control reach temperature changes across harvest ($\Delta T_{1W,2W} = -0.2\,^{\circ}$C). Site 7854 also possessed the second smallest WD value among all sites. This combination resulted in a relatively high rate of reduction in the temperature change, as seen in Figure 3. The NLC model shows us that the outlying behaviour of this site was caused by this high rate of change coupled with a relatively long transit time for this site, due to a combination of long downstream reach length ($L = 305$ m) and third lowest gradient ($G = 0.023$). This result highlights the potential utility of the NLC model in predicting which sites may exhibit abnormal behaviour in response to harvest, before harvest ever begins.

In order to further leverage the predictive power of the NLC model, we examine how the across-harvest temperature change depends on the distance from the harvest reach, when that downstream change is caused purely by a change in the harvest reach temperature, in the absence of any climatic fluctuations. For this case, the change in equilibrium temperature is zero, leaving only the first term in the model:

$$\Delta T4W(x) = \Delta T3W e^{-\varphi \frac{x}{WDG^{1/2}}} \tag{16}$$

Intuitively, larger harvest reach temperature changes will lead directly to larger downstream temperature changes, as can be seen from Equation (16). In order to focus on site-specific downstream behaviour, we normalize the downstream change to the harvest reach change and thus define the distance dependent ratio of $\Delta T4W$ to $\Delta T3W$ as $R(x)$. For the case of 0 change in equilibrium temperature, $R(x)$ has the form

$$R(x) = \frac{\Delta T4W}{\Delta T3W} = e^{-\varphi \frac{x}{WDG^{1/2}}} \tag{17}$$

Using average values for G and WD will allow us to estimate a characteristic behaviour of the sites in our study. The solid green line in Figure 4 shows $R(x)$ for the average values of $G = 0.047$ and $WD = 0.53$ m^2. We see that for these average values, the across-harvest-year change in downstream temperature drops to 56% of that

Copyright © 2015 John Wiley & Sons, Ltd.

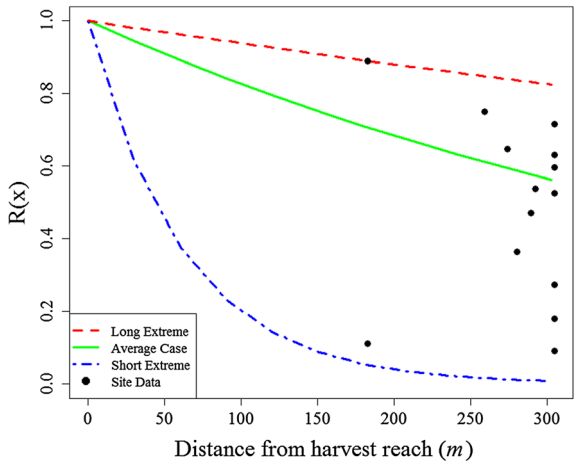

Figure 4. Calculated ratio of harvest reach and downstream temperature changes in the absence of stream equilibrium temperature fluctuations as a function of distance from harvest reach using maximum (red) minimum (blue) and average (green) measured values of G (0.047) and WD (0.53 m^2). Dots show this value calculated using site-specific values of G, WD and L for each site. In all cases, $\Delta T4W_{eq} = 0$ °C and model parameter values were $\varphi = 2.2 \times 10^{-4}$ m, $\beta = 1.1$

change occurring in the harvest reach after 300 m. These calculations are qualitatively supported by the result of the linear fit, which suggests a statistical 50% reduction in temperature change after ≈300 m. However, $R(x)$ is exponentially sensitive to G and WD, and consequently, the average or statistical result cannot be used to accurately describe the behaviour of a specific site, hence the utility of the NLC model.

In order to estimate bounding behaviours for the distance dependence of the change in temperature for sites similar to those in this study, we combined the extreme values of G and WD measured from all sites and used these in the model. The maximum measured values are $G = 0.11$ and $WD = 1.0$ m^2, and the minimal values are $G = 0.01$ and $WD = 0.12$ m^2. The bounding behaviours calculated from these two value sets are shown in Figure 4. For the long-distance extreme case, the downstream temperature change measured 300 m from the end of the harvest reach would be 82% of the temperature change that occurred at the end of the harvest reach ($R(x) = 0.82$). For the short-distance extreme case, $R(x)$ is less than 1% after 300 m. Values of $R(x = L)$ calculated using the specific stream property values and reach lengths at each study site are also shown for comparison with the bounding behaviour curves. We see that the behaviour of one site lies directly on the boundary curve because that site possessed the maximum measured values for both G and WD.

In order to examine the specific effects of a change to the downstream equilibrium temperature, $\Delta T4W_{eq}$, on the downstream temperature response, we calculate $R(x)$ for theoretical example cases when $\Delta T4W_{eq} \neq 0$. In this case, the form for $R(x)$ is more complex:

$$R(x) = e^{-\varphi \frac{L}{WDG^{1/2}}} + \frac{\beta \Delta T_{1W,2W}}{\Delta T3W}\left[1 - e^{-\varphi \frac{L}{WDG^{1/2}}}\right] \quad (18)$$

We see that calculating $R(x)$ for $\Delta T4W_{eq} \neq 0$ requires input values for $\Delta T3W$ and $\Delta T4W_{eq}$. As seen in Table I, the range of values for $\Delta T4W_{eq}$ extracted from the model was approximately −0.4 to 0.4 °C. Figure 5 shows $\Delta T4W$ calculated for $\Delta T4W_{eq}$ equal to the end-range values of −0.4 and 0.4 °C, each for two cases of the harvest-reach temperature change within the range typically observed, namely, 1 and 3 °C (solid green lines). We see that changes to $\Delta T4W_{eq}$ within this range do not significantly affect the dependence of $\Delta T4W$ on distance relative to the precision of typical temperature measurements. However, we see that integrated over distances of 300 m these relatively slight changes in distance dependence may affect the value of $\Delta T4W$ by detectable levels (≈ 0.3 °C).

Sensitivity to specific stream properties

The wide range of downstream behaviours encompassed by the bounding behaviours exemplifies the exponential sensitivity of $R(x)$ to G and WD. These sensitivities are illustrated with greater detail in Figures 6 and 7, which show $R(x)$ as a function of G and WD, respectively, at the reach end ($x = 300$ m) and half-length ($x = 150$ m) for comparison. We see that the slopes of these curves are significant within the range of measured values (indicated by the shaded grey regions in Figures 6 and 7) for these stream properties, and thus, the measured behaviour is highly sensitive to these properties. This analysis indicates that blanket statements about distance required for stream temperature to return to pre-harvest

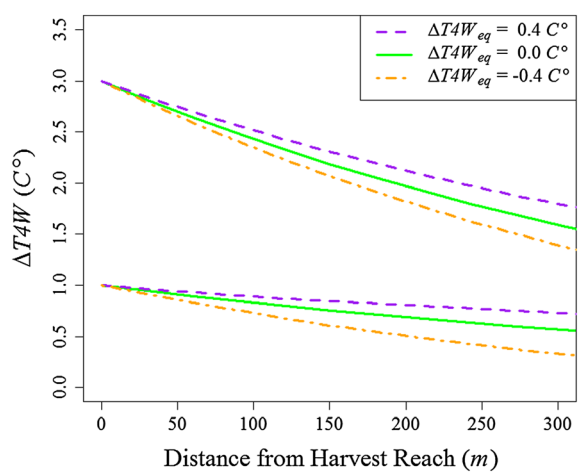

Figure 5. Distance dependence of $\Delta T4W$ calculated for $\Delta T4W_{eq}$ values of 0, −0.4 and 0.4 °C for the example cases of $\Delta T3W = 1$ °C and $\Delta T3W = 3$ °C. The legend designates these values used to produce each curve in the format ($\Delta T3W$, $\Delta T4W_{eq}$). The average of measured values for G (0.047) and WD (0.53 m^2) was used, and model parameter values were $\varphi = 2.2 \times 10^{-4}$ m, $\beta = 1.1$

Copyright © 2015 John Wiley & Sons, Ltd.

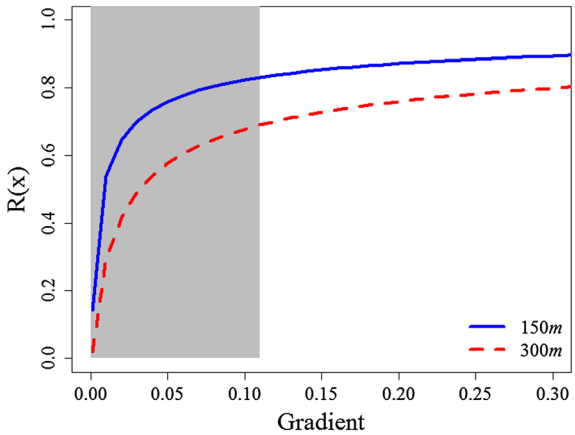

Figure 6. Calculated ratio of downstream to harvest reach temperature changes at distances of 150 and 300 m downstream from harvest reach as a function of downstream gradient in the absence of natural stream fluctuations. In all cases, the average measured values for WD (0.53 m^2) were used, $\Delta T4W_{eq} = 0$ °C, and model parameter values were $\varphi = 2.2 \times 10^{-4}$ (m), $\beta = 1.1$. The grey shaded area indicates the range of gradient values measured in this study

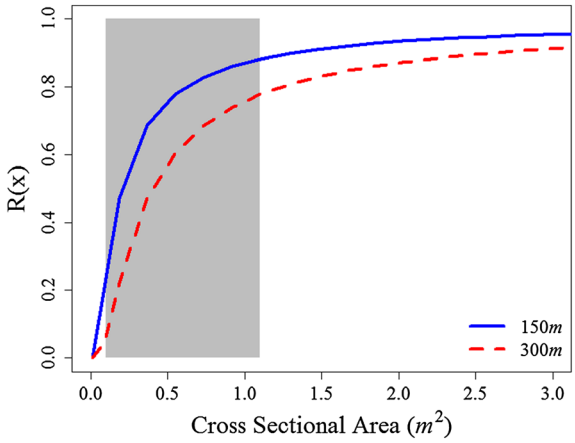

Figure 7. Calculated ratio of downstream to harvest reach temperature changes at distances of 150 and 300 m downstream from harvest reach as a function of downstream cross-sectional area in the absence of stream equilibrium temperature fluctuations. In all cases, the average measured values for WD (0.53 m^2) were used, $\Delta T4W_{eq} = 0$ °C, and model parameter values were $\varphi = 2.2 \times 10^{-4}$ (m), $\beta = 1.1$. The grey shaded area indicates the range of cross-sectional area values measured in this study

value ($\Delta T4W <$ thermistor resolution) and use of regional average or non-local variable values to model site-specific behaviour may lead to miscalculations.

For the narrow range of downstream shade factor values measured in the study streams, we found that shade had no significant effect on the behaviour of the model. Owing to all measured values of S being near one, modelling α' as proportional to or inversely proportional to S does not produce significantly different results in the performance of the model or the values of the parameters determined from fitting the model to data. Thus, the downstream shade data are not sufficiently ranged to

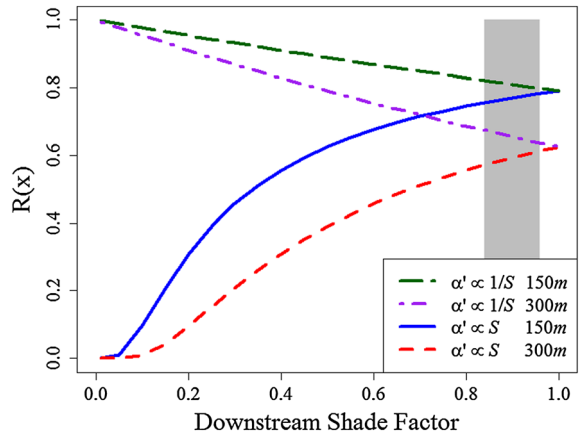

Figure 8. Calculated ratio of downstream to harvest reach temperature changes at distances of 150 and 300 m downstream from harvest reach as a function of downstream shade in the absence of stream equilibrium temperature fluctuations. Curves produced using both $\alpha' \propto 1/S$ and $\alpha' \propto S$ models are shown. Average measured values of G (0.047) and WD (0.53 m^2) were used. In all cases, $\Delta T4W_{eq} = 0$ °C, and model parameter values were stream equilibrium temperature fluctuations, $\beta = 1.1$. The grey shaded area indicates the range of shade factor values measured in this study

allow for evaluation of a shade component to model. Figure 8 shows $R(x = 150 \text{ m})$ and $R(x = 300 \text{ m})$ for both model types, $\alpha' \propto 1/S$ and $\alpha' \propto S$. We see that within the range of S values measured (indicated by the shaded grey region in Figure 8), the slope of these curves is small relative to that in Figures 6 and 7, which demonstrates the relative insensitivity of the model to the shade variable within that range. The success of the model at describing the data despite the model insensitivity to S indicates that for streams with relatively uniform and undisturbed riparian conditions downstream of harvest (high shade and shelter), the values of G and WD will primarily drive the variations in downstream temperature response

CONCLUSIONS

For the forested streams in our study, the model suggests that, on average, pre- to post-changes in downstream temperature exist at roughly 50% of those changes in the harvest reach after ≈300 m downstream, but that they do not persist indefinitely. The model also indicates that variation in stream morphology can lead to significant variability in this downstream temperature response to harvest, and it allowed us to estimate limiting-case behaviours. We estimated that for streams similar to those in this study, the across-harvest-year temperature change ≈300 m downstream of the harvest reach can range from 82% to less than 1% of the change in the harvest reach, in the absence of major tributaries, with a significant portion of that wide variation being predictable if a few specific and easily measureable stream properties are known.

Copyright © 2015 John Wiley & Sons, Ltd.

Additional application of NLC modelling methods to stream temperature data should help to improve the NLC model accuracy and determine the range of stream, environmental and treatment conditions under which the NLC model is valid and accurate. For example, data from a set of many temperature probes within individual reaches would allow us to fit the Lagrangian NLC model to the Eulerian temperature data at each site and determine reach-specific values for the model free parameters φ and β. Comparison of these parameter values to measured stream properties may allow us to identify those properties with greatest influence on φ and β so that we might model these values directly and reduce the number of free parameters in the NLC model and improve its accuracy. Analysis of data from a set of streams with a wider range of downstream shade values might permit the addition and validation of a downstream shade component in the model and allow for investigation of a minimum shade threshold required for the NLC model to maintain accuracy. Finally, analysis of data from streams with a wider range of morphologies and environments would test the generality of the NLC model and provide a greater range of input variables against which to test, refine and improve an NLC-based model.

ACKNOWLEDGEMENTS

This work was supported by the Oregon Department of Environmental Quality, the Oregon Department of Forestry and Weyerhaeuser Company NR. We thank the RipStream Technical Committee for helpful discussion. Data are available free of charge from the Oregon Department of Forestry's Forest Practices Research & Monitoring Program (http://www.oregon.gov/ODF/Pages/index.aspx). This project has been funded wholly or in part by the United States Environmental Protection Agency (EPA) under assistance agreement C9-00045112 to the Oregon Department of Environmental Quality. The contents of this document do not necessarily reflect the views and policies of the Environmental Protection Agency, nor does mention of trade names or commercial products constitute endorsement or recommendation for use.

REFERENCES

Adams TN, Sullivan K. 1989. *The Physics of Forest Stream Heating: A Simple Model. TFW-WQ3-90-007*. Washington Department of Natural Resources: Olympia, Washington; 30.

Baillie BR, Collier KJ, Nagels J. 2005. Effects of forest harvesting and woody debris removal on two Northland streams, New Zealand. *New Zealand Journal of Marine and Freshwater Research* **39**(1): 1–15.

Bogan T, Mohseni O, Stefan HG. 2003. Stream temperature–equilibrium temperature relationship. *Water Resources Research* **39**: 1245. DOI:10.1029/2003WR002034.

Boyd M, Kasper B. 2003. "*Analytical Methods for Dynamic Open Channel Heat and Mass Transfer: Methodology for Heat Source Model Version 7.0*." Oregon Department of Environmental Quality: Portland, Oregon. Web site: http://www. deq. state. or. us/wq/TMDLs/tools. htm

Brown GW. 1969. Predicting temperatures of small streams. *Water Resources Research* **5**: 68–75.

Brown GW, Krygier JT. 1970. Effect of clear cutting on stream temperature. *Water Resources Research* **6**: 1133–1139.

Brown GW, Swank GW, Rothacher J. 1971. Water temperature in the steamboat drainage, Pacific Northwest forest and Range Expt. Sta., Forest Service, U.S. Department of Agriculture, Portland. Oregon. Research Paper PNW-1 19. 17 p.

Burnham KP, Anderson DR. 2002. *Model Selection and Multimodel Inference: A Practical Information-Theoretic Approach*, 2nd edition. Springer-Verlag: New York; 488.

Caissie D. 2006. The thermal regime of rivers: a review. *Freshwater Biology* **51**13891406: . DOI:10.1111/j.1365-2427.2006.01597.x.

Caldwell JE, Doughty K, Sullivan K. 1991. *Evaluation of downstream temperature effects on type 4/5 waters, Timber/Fish/Wildlife Report #TFW-WQ5-91-004*. Washington Dept. of Natural Resources: Olympia, WA 71 p.

Cole E, Newton M. 2013. Influence of streamside buffers on stream temperature response following clear-cut harvesting in western Oregon. *Canadian Journal of Forest Research* **43**: 993–1005. DOI:10.1139/cjfr-2013-0138.

DaSilva A, Xu YJ, Ice G, Beebe J, Stich R. 2013. Effects of timber harvesting with best management practices on ecosystem metabolism of a low gradient stream on the United States Gulf Coastal Plain. *Water (Switzerland)* **5**(2): 747–766.

Dent L, Vick D, Abraham K, Schoenholtz S, Johnson S. 2008. Summer temperature patterns in headwater streams of the Oregon Coast Range. *Journal of the American Water Resources Association* **44**: 803–813. DOI:10.1111/j.1752-1688.2008.00204.x.

Doyle MW, Ensign SH. 2009. Alternative reference frames in river system science. *BioScience* **59**(6): 499–510.

Edinger JE, Duttweiler DW, Geyer JC. 1968. The response of water temperatures to meteorological conditions. *Water Resources Research* **4**: 1137–1143. DOI:10.1029/WR004i005p01137.

Garner G, Malcolm IA, Sadler JP, Hannah DM. 2014. What causes cooling water temperature gradients in forested stream reaches? *Hydrology and Earth System Sciences Discussions* **11**(6): 6441–6472.

Gomi T, Moore RD, Dhakal AS. 2006. Headwater stream temperature response to clear-cut harvesting with different riparian treatments, coastal British Columbia, Canada. *Water Resources Research* **42**W08437 DOI:10.1029/2005WR004162.

Gravell JA, Link TE. 2007. Influence of timber harvesting on headwater peak stream temperatures in a Northern Idaho watershed. *Forest Science* **53**: 189–205.

Gray JRA, Edington JM. 1969. Effect of woodland clearance on stream temperature. *Journal of the Fisheries Board of Canada* **26**(2): 399–403.

Groom JD, Dent L, Madsen L. 2011a. Stream temperature change detection for state and private forests in the Oregon Coast Range. *Water Resources Research* **47**W01501 DOI:10.1029/2009WR009061.

Groom JD, Dent L, Madsen L, Fleuret J. 2011b. Response of Western Oregon (U.S.A.) stream temperatures to contemporary forest management. *Forest Ecology and Management* **262**: 1618–1629. DOI:10.1016/j.foreco.2011.07.012.

Hairston-Strang AB, Adams PW, Ice GG. 2008. The Oregon forest practices act and forest research. In *Hydrological and Biological Responses to Forest Practices*. Springer: New York; 95–113.

Janisch JE, Wondzell SM, Ehinger WJ. 2012. Headwater stream temperature: interpreting response after logging, with and without riparian buffers, Washington, USA. *Forest Ecology and Management* **270**: 302–313. DOI:10.1016/j.foreco.2011.12.035.

Johnson SL. 2004. Factors influencing stream temperatures in small streams: substrate effects and a shading experiment. *Canadian Journal of Fisheries and Aquatic Sciences* **61**: 913–923. DOI:10.1139/f04-040.

Johnson MF, Wilby RL. 2015. Seeing the landscape for the trees: metrics to guide riparian shade management in river catchments. *Water Resources Research* **51**(5): 3754–3769.

Kaufmann PR, Robison EG. 1998. Environmental Monitoring and Assessment Program – Surface waters: field operations and methods

Copyright © 2015 John Wiley & Sons, Ltd.

for measuring the ecological condition of wadeable streams, pp 77–118 In: EPA/620/R-94/004F. Office of Research and Development, U.S. Environmental Protection Agency, Washington, D.C.

Kibler KM, Skaugset A, Ganio LM, Huso MM. 2013. Effect of contemporary forest harvesting practices on headwater stream temperatures: initial response of the Hinkle Creek catchment, Pacific Northwest, USA. *Forest Ecology and Management* **310**: 680–691. DOI:10.1016/j.foreco.2013.09.009.

Moore RD, Spittlehouse DL, Story A. 2005. Riparian microclimate and stream temperature response to forest harvesting: a review. *Journal of the American Water Resources Association* **41**: 813–834. DOI:10.1111/j.1752-1688.2005.tb03772.x.

Rex JF, Maloney DA, Krauskopf PN, Beaudry PG, Beaudry LJ. 2012. Variable-retention riparian harvesting effects on riparian air and water temperature of sub-boreal headwater streams in British Columbia. *Forest Ecology and Management* **269**: 259–270. DOI:10.1016/j.foreco.2011.12.023.

Roth TR, Westhoff MC, Huwald H, Huff JA, Rubin JF, Barrenetxea G, Vetterli M, Parriaux A, Selker JS, Parlange MB. 2010. Stream temperature response to three riparian vegetation scenarios by use of a distributed temperature validated model. *Environmental Science & Technology* **44**(6): 2072–2078.

Rutherford JC, Marsh NA, Davies PM, Bunn SE. 2004. Effects of patchy shade on stream water temperature: how quickly do small streams heat and cool? *Marine and Freshwater Research* **55**(8): 737–748.

Story A, Moore RD, Macdonald JS. 2003. Stream temperatures in two shaded reaches below cutblocks and logging roads: downstream cooling linked to subsurface hydrology. *Canadian Journal of Forest Research* **33**: 1383–1396. DOI:10.1139/x03-087.

Subramanya V. 2009. *Flow in Open Channels*, 3rd edition. New Delhi: McGraw-Hill.

Sugimoto S, Nakamura F, Ito A. 1997. Heat budget and statistical analysis of the relationship between stream temperature and riparian forest in the Toikanbetsu River basin, northern Japan. *Journal of Forest Research* **2**: 103–107. DOI:10.1007/BF02348477.

Valverde T, Silvertown J. 1997. Canopy closure rate and forest structure. *Ecology* **78**: 1555–1562. DOI:10.2307/2266148.

Zwieniecki M, Newton M. 1999. Influence of streamside cover and stream features on temperature trends in forested streams of western Oregon. *Western Journal of Applied Forestry* **14**: 106–113.

Copyright © 2015 John Wiley & Sons, Ltd.